Proceedings of ASME:
2003 ASME Summer Heat Transfer Conference
July 21-23, 2003, Las Vegas, Nevada

HT2003-40289

ANALYSIS OF MELTING IN A MIXED METAL POWDER BED WITH FINITE THICKNESS SUBJECTED TO CONSTANT HEAT FLUX HEATING

Tiebing Chen and Yuwen Zhang
Department of Mechanical Engineering
New Mexico State University
Las Cruces, NM 88003
zhangy12@asme.org

ABSTRACT

Melting of a subcooled powder bed with the finite thickness that contains a mixture of two metal powders with significantly different melting points is investigated analytically. Shrinkage induced by melting is taken into account in the physical model. The temperature distributions in the liquid and solid phases were obtained using an exact solution and an integral approximate solution, respectively. The effects of porosity, Stefan number, and subcooling on the surface temperature and solid-liquid interface are also investigated. The present work built solid foundation to investigate the complex three-dimensional selective laser sintering (SLS) process.

NOMENCLATURE

c_p specific heat [$Jkg^{-1}K^{-1}$]

h_{sl} latent heat of melting or solidifation [$J\ kg^{-1}$]

H_0 The thickness of the powder bed

k thermal conductivity [$W\ m^{-1}K^{-1}$]

K_g dimensionless thermal conductivity of gas

K_S dimensionless effective thermal conductivity of unsintered powder

q_{in} heat flux [$W\ m^{-2}$]

s solid-liquid interface location [m]

S dimensionless solid-liquid interface location

s_0 location of liquid surface [m]

S_0 dimensionless location of liquid surface

Sc subcooling parameter

Ste Stefan number

t time [s]

T temperature [K]

w velocity of liquid phase [$m\ s^{-1}$]

W dimensionless velocity of the liquid phase

z coordinate [m]

Z dimensionless coordinate

Greek symbols

α thermal diffusivity [$m^2\ s^{-1}$]

$\overline{\alpha}$ dimensionless thermal diffusivity

β the parameter to distinguish between two melting cases

δ thermal penetration depth [m]

Δ dimensionless thermal penetration depth

ε volume fraction of gas(es) (porosity for unsintered powder)

θ dimensionless temperature

ρ density [$kg\ m^{-3}$]

τ dimensionless time

ϕ volume fraction of the low melting point powder in the powder mixture

Subscripts

g gas

i initial

l liquid phase

m melting point

p sintered part

s unsintered solid (mixture of two solid powders)

1. INTRODUCTION

Selective Laser Sintering (SLS) is an emerging technology of Solid Freeform Fabrication (SFF) that 3-D parts are built with CAD data [1]. In fabrication of near full density objects from metal powder, SFF is realized via melting and resolidification that are induced by a directed laser beam. A powerful heat transfer model that predicts the temperature distribution in the process of melting plays an important role since it has significant impact on the final quality of parts.

Melting in SLS of metal powder is significantly different from the normal melting since the volume fraction of the gas in the powder decreases from a value as large as 0.5 to nearly zero after melting. Therefore, a significant density change of the powder bed accompanies the melting process. Fundamentals of melting and solidification have been investigated extensively and detailed reviews are available in the literatures [2, 3]. Melting and solidification in 1-D semi-infinite body with density change under the boundary condition of the first kind have been investigated by Zckert and Drake [4], Crank [5], Carslaw and Jaeger [6] and Charach and Zarmi [7]. It should be noted that melting during SLS occurs under the boundary condition of specified heat flux instead of specified temperature. Zhang et al. [8] investigated the melting problem in a subcooled semi-infinite region subjected to constant heat flux heating. Goodman and Shea [9] studied melting and solidification in the finite slab under a specified heat flux by using the heat balance integral method. Zhang et al. [10] solved melting in a finite slab with the boundary condition of the second kind by using a semi-exact method. Shrinkage formation due to density change during the solidification process in 2-D cavity was investigated numerically by Kim and Ro [11], who conducted that the density change played a more important role than the convection in the solidification process.

In order to avoid the so called "balling" phenomenon, SLS using the metal powder mixture with two kinds of powders which possess significantly different melting points was suggested by Manzur et al. [12] and Bunnell [13]. Only the low melting point powder melts and resolidifies during the SLS process. Zhang and Faghri [14] analytically solved a one-dimensional melting problem in a semi-infinite powder bed containing a mixture of the powder subjected to a constant heat flux heating. Effects of the porosity of the solid phase, initial subcooling parameter and dimensionless thermal conductivity of gas were investigated. Since SLS of the metal powder is actually a layer-by-layer process, it is necessary to investigate melting in a mixed metal powder bed with the finite thickness during the SLS process. In this paper, melting of the mixed powder bed with finite thickness subjected constant heat flux heating will be investigated.

2. PHYSICAL MODEL

The physical model of the melting problem is shown in Fig. 1. A powder bed with finite thickness contains two metal powders with significantly different melting points. The initial temperature of the powder bed is below the melting point of the low melting point powder. At time $t = 0$, a constant heat flux, q_{in}, is suddenly applied to the top surface of the powder bed, and the bottom surface of the powder bed is assumed to be adiabatic. Since the initial temperature of the powder bed is below the melting point of the low melting point powder, melting of the low melting point powder does not start simultaneously with the beginning of the heating. Only after a finite period of time of preheating, in which the surface temperature of the powder reaches the melting point of the low melting point powder, will the melting start. The powder with the high melting point will never melt during the entire process. Therefore, the problem can be subdivided into two problems: one is the heat conduction during preheating and the other one is melting.

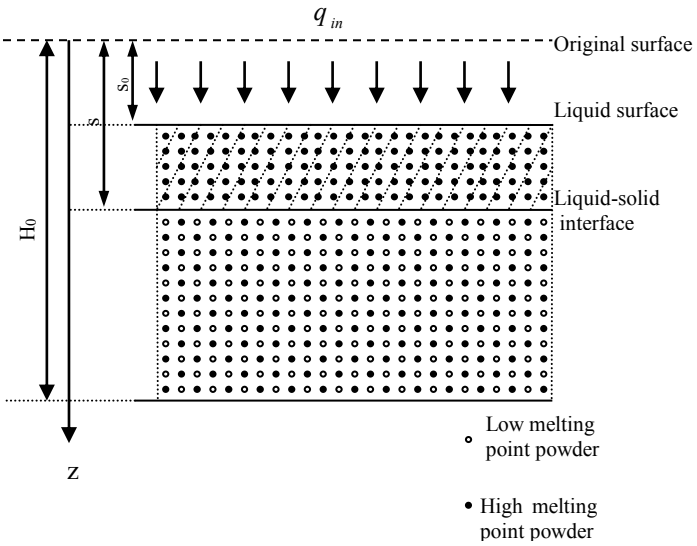

Fig1. Physical model

2.1 Duration of preheating

During preheating, the pure conduction heat transfer occurs in the powder mixture. The governing equation and the corresponding initial and boundary conditions for the preheating problem are

$$\alpha_s \frac{\partial^2 T_s}{\partial z^2} = \frac{\partial T_s}{\partial t}, \quad 0 < z < H_0, \ t < t_m \tag{1}$$

$$T = T_i, \quad 0 < z < H_0, \ t = 0 \tag{2}$$

$$-k_s \frac{\partial T_s}{\partial z} = q_{in}, \quad z = 0, \ t < t_m \tag{3}$$

$$\frac{\partial T_s}{\partial z} = 0, \quad z = H_0, \ t < t_m \tag{4}$$

2.2 Melting

After melting starts, the governing equation in the liquid phase is

$$\alpha_l \frac{\partial^2 T_l}{\partial z^2} = \frac{\partial T_l}{\partial t} + w \frac{\partial T_l}{\partial z}, s_0 < z < s(t), \ t > t_m \tag{5}$$

where w is the velocity of liquid surface induced by the shrinkage. Since the liquid is incompressible, the shrinkage velocity w is

$$w = \frac{ds_0}{dt}, \quad s_0 < z < s(t), \ t > t_m \tag{6}$$

Equation (5) is subjected to the following boundary condition

$$-k_l \frac{\partial T_l}{\partial z} = q_{in}, \quad z = 0, \ t > t_m \tag{7}$$

The governing equation for the solid phase and its corresponding boundary conditions are

$$\alpha_s \frac{\partial^2 T_s}{\partial z^2} = \frac{\partial T_s}{\partial t}, \quad s(t) < z < H_0, \ t > t_m \tag{8}$$

$$\frac{\partial T_s}{\partial z} = 0, \quad z = H_0, \ t > t_m \tag{9}$$

The temperature at the solid-liquid interface satisfies

$$T_l(z,t) = T_s(z,t) = T_m, \quad z = s(t), \ t > t_m \tag{10}$$

The energy balance at the solid-liquid interface is

$$k_s \frac{\partial T_s}{\partial z} - k_l \frac{\partial T_l}{\partial z} = (1-\varepsilon_s)\phi\rho_l h_{sl} \frac{ds}{dt}, \ z = s(t), \ t > t_m \tag{11}$$

Based on the conservation of mass at the solid-liquid interface, the shrinkage velocity, w, and the solid-liquid interface velocity, ds/dt, have the following relationship [14]

$$w = \frac{\varepsilon_s - \varepsilon_l}{1-\varepsilon_l} \frac{ds}{dt} \tag{12}$$

2.3 Non-dimensional governing equations

By defining the following dimensionless variables

$$K_s = \frac{k_s}{k_p(1-\varepsilon_s)}, \ K_g = \frac{k_g}{k_p}, \ \bar{\alpha}_s = \frac{\alpha_s}{\alpha_p}, \ Ste = \frac{q_{in}H}{\phi\rho_l h_{sl}\alpha_p}, \ S_0 = \frac{s_0}{H}$$

$$Sc = \frac{(\rho c_p)_p (T_m - T_i)}{\phi\rho_l h_{sl}}, \ \tau = \frac{\alpha_p t}{H^2}, \ S = \frac{s}{H}, \ \Delta = \frac{\delta}{H}, \ W = \frac{w \cdot H}{\alpha_p}$$

$$\theta_l = \frac{(\rho c_p)_p (T_l - T_m)}{\phi\rho_l h_{sl}}, \ \theta_s = \frac{(\rho c_p)_p (T_s - T_m)}{\phi\rho_l h_{sl}}, \tag{13}$$

The non-dimensional governing equation and the corresponding initial and boundary conditions for the preheating problem are as following.

$$\frac{\partial^2 \theta_s}{\partial Z^2} = \frac{1}{\bar{\alpha}_s} \cdot \frac{\partial \theta_s}{\partial \tau}, \quad 0 < Z < 1, \ \tau < \tau_m \tag{14}$$

$$\theta = \theta_i, \quad 0 < Z < 1, \ \tau = 0 \tag{15}$$

$$\frac{\partial \theta_s}{\partial Z} = -\frac{Ste}{K_s(1-\varepsilon_s)}, \quad Z = 0, \ \tau < \tau_m \tag{16}$$

$$\theta_s = -Sc, \quad Z = \Delta, \ \tau < \tau_m \tag{17}$$

$$\frac{\partial \theta_s}{\partial Z} = 0, \quad Z = \Delta, \ \tau < \tau_m \tag{18}$$

For melting, the non-dimensional equation and corresponding boundary conditions are

$$\frac{\partial^2 \theta}{\partial Z^2} = \frac{\partial \theta}{\partial \tau} + W \frac{\partial \theta}{\partial Z}, S_0 < Z < S(\tau), \tau > \tau_m \tag{19}$$

$$W = \frac{dS_0}{d\tau} \quad S_0 < Z < S(t), \ t > t_m \tag{20}$$

$$\frac{\partial \theta}{\partial Z} = -\frac{Ste}{1-\varepsilon_l}, \quad Z = S_0, \tau > \tau_m \tag{21}$$

$$\frac{\partial^2 \theta}{\partial Z^2} = \frac{1}{\bar{\alpha}_s} \cdot \frac{\partial \theta}{\partial \tau}, \quad S(\tau) < Z < 1, \ \tau > \tau_m \tag{22}$$

$$\frac{\partial \theta}{\partial Z} = 0, \quad Z = 1, \ \tau > \tau_m \tag{23}$$

$$\theta_l(Z,\tau) = \theta_s(Z,\tau) = 0, Z = S(\tau), \ \tau > \tau_m \tag{24}$$

$$K_s \frac{\partial \theta_s}{\partial Z} - \frac{1-\varepsilon_l}{1-\varepsilon_s} \frac{\partial \theta_l}{\partial Z} = \frac{dS}{d\tau}, Z = S(\tau), \ \tau > \tau_m \tag{25}$$

$$W = \frac{\varepsilon_s - \varepsilon_l}{1-\varepsilon_l} \frac{dS}{d\tau}, \quad S_0 < Z < S(t), \ t > t_m \tag{26}$$

3. APPROXIMATE SOLUTIONS

When the top surface of the mixed metal powder bed is subjected to a constant flux heating, the heat flux will penetrate through the top surface and conduct downward. The thickness at which the heat flux arrives at an instant time is defined as the thermal penetration depth, beyond which there is no heat conduction. Goodman and Shea [9] introduced a parameter, $\beta = q_{in}H/[2k_s(T_m - T_i)]$, to classify two cases of melting in a finite slab. When β is greater than 1, the top surface temperature reaches the melting point faster than the thermal penetration depth approaches the bottom surface, indicating that a shorter preheating time is needed. If β is less than 1, the surface temperature is still below the melting point when the thermal penetration depth has reached the bottom surface. Preheating continues until the top surface temperature reaches the melting point of low melting point powder.

The parameter β can also be expressed using non-dimensional parameters defined in eq. (13), i.e., $\beta = Ste/[2K_s Sc(1-\varepsilon_s)]$. It can be seen that the value of β is determined by four basic non-dimensional parameters: Stefan

number Ste, subcooling parameter Sc, effective thermal conductivity of the solid phase K_s and volume fraction of gas ε_s in the solid phase. Preheating and melting based on different cases of β will be discussed respectively as following.

3.1 Preheating

3.1.1 $\beta < 1$

The heat-balance integral method is employed here. Integrating the heat-conduction equation (14), with respect to Z from 0 to Δ, the integral equation is obtained.

$$\left[\frac{\partial \theta_s}{\partial Z}(\Delta,\tau) - \frac{\partial \theta_s}{\partial Z}(0,\tau)\right] = \frac{1}{\bar{\alpha}_s}\frac{d}{d\tau}(\Theta + Sc\Delta) \tag{27}$$

where

$$\Theta = \int_0^{\Delta} \theta(Z,\tau)\,dZ \tag{28}$$

It is assumed that $\theta(Z,\tau)$ is of the form

$$\theta_s(Z,\tau) = a + bZ + cZ^2 \tag{29}$$

where a, b, and c are unspecified constants. Equation (29) must satisfy boundary conditions specified by eqs. (16-18). Substituting eq. (29) into eqs. (16-18), the constants in eq. (29) can be determined and eq. (29) becomes

$$\theta_s(Z,\tau) = -Sc + \frac{Q}{2K_s\Delta(1-\varepsilon_s)}(\Delta - Z)^2 \tag{30}$$

Substituting eq. (30) into eq. (28) yields

$$\Theta = \frac{Ste}{6K_s(1-\varepsilon_s)}\cdot\Delta^2 - Sc\Delta \tag{31}$$

Substituting eqs. (16-18) and (30-31) into eq. (27), an ordinary differential equation about the thermal penetration depth, Δ, is obtained. The dimensionless thermal penetration depth can be obtained by solving the ordinary differential equation and the result is

$$\Delta = (6\cdot\bar{\alpha}_s\cdot\tau)^{1/2} \tag{32}$$

When the thermal penetration depth reaches the bottom surface, i.e., $\Delta = 1$, the temperature distribution in the powder bed is

$$\theta_s(Z,\tau) = -Sc + \frac{Ste}{2K_s(1-\varepsilon_s)}(1-Z)^2, \tag{33}$$

which becomes the initial condition of the next stage of preheating. After the thermal penetration depth reaches to the bottom, the problem becomes a conduction problem in a finite slab. In a manner analogous to that described in the foregoing, the heat-balance integral method is also used to solve the conduction problem. The temperature in the powder bed after the thermal penetration depth reached the bottom is

$$\theta_s(Z,\tau) = -Sc + \frac{Ste}{2K_s(1-\varepsilon_s)}(1-Z)^2 + \frac{Ste\cdot\bar{\alpha}_s}{K_s(1-\varepsilon_s)}(\tau - \tau_{\Delta=1})$$
$$0 < Z < 1, \tau_{\Delta=1} < \tau < \tau_m \tag{34}$$

The preheating time, τ_m, can be obtained by setting $\theta(0,\tau) = 0$ in eq. (34), i.e.,

$$\tau_m = \frac{1}{\bar{\alpha}_s}\left[-\frac{1}{3} + \frac{1}{2\beta}\right] \tag{35}$$

The temperature distribution at $\tau = \tau_m$ is given by

$$\theta_s(Z,\tau_m) = -\frac{Ste}{2K_s(1-\varepsilon_s)}[1-(1-Z)^2] \tag{36}$$

which is the initial condition for melting.

3.1.2 $\beta > 1$

When β is greater than 1, melting starts before the penetration depth reaches to the bottom and therefore, the preheating time, τ_m, corresponding thermal penetration depth, Δ_m, and temperature distribution at time τ_m are [14]

$$\tau_m = \frac{2}{3}(1-\varepsilon_s)^2 K_s^2 Sc^2\cdot\frac{1}{Ste^2\bar{\alpha}_s} \tag{37}$$

$$\Delta_m = 2(1-\varepsilon_s)K_s Sc\cdot\frac{1}{Ste} \tag{38}$$

$$\theta_s(Z,\tau) = Sc\left[\left(1-\frac{Z}{\Delta_m}\right)^2 - 1\right], \quad Z > 0, \quad \tau = \tau_m \tag{39}$$

$$\theta_s(0,\tau) = -Sc + Ste\cdot\sqrt{6\alpha_s\tau}\,/[2\cdot K_s\cdot(1-\varepsilon_s)],$$
$$Z = 0, \quad 0 < \tau < \tau_m \tag{40}$$

where eq. (40) is the surface temperature on the top of the powder bed.

3.2 Solution of melting

3.2.1 Temperature distribution in the liquid

The melting starts when the surface temperature reaches the melting point of the low melting point powder. A liquid layer is formed as the result of melting. The temperature distribution in

the liquid phase does not depend on the value of β . It can be obtained by an exact solution of eqs. (19-21) and (24) [14], i.e.

$$\theta_l(Z,\tau)=\frac{2Ste\sqrt{\tau-\tau_m}}{1-\varepsilon_l}\left[ierfc\left(\frac{Z-S_0}{2\sqrt{\tau-\tau_m}}\right)-ierfc\left(\frac{S-S_0}{2\sqrt{\tau-\tau_m}}\right)\right] \tag{41}$$

where S_0 is dimensionless location of liquid surface.

3.2.2 Temperature distribution in the solid when $\beta<1$

Thermal penetration depth reached the bottom of the powder bed before melting is started. The integral approximate solution can be employed to obtain the temperature distribution in the solid phase. Integrating eq. (22) with respect to Z in the interval of (S, 1), one can obtain

$$-\frac{\partial\theta_s}{\partial Z}\Big|_{Z=S}=\frac{1}{\bar{\alpha}_s}\frac{d\Theta}{d\tau} \tag{42}$$

where

$$\Theta=\int_S^1\theta_S dZ \tag{43}$$

It is assumed that the temperature distribution in the solid phase is,

$$\theta_s(Z,\tau)=a+b(1-Z)+c(1-Z)^2 \tag{44}$$

The unspecified constants b and c in eq. (44) can be eliminated by using eqs. (23-24) and eq. (44) becomes

$$\theta_s(Z,\tau)=a\left[1-\left(\frac{1-Z}{1-S}\right)^2\right] \tag{45}$$

Substituting eq. (45) into eqs.(43- 42), an ordinary differential equation about a is obtained

$$\frac{da}{d\tau}+\frac{3\bar{\alpha}}{2(1-S)^2}a=0 \tag{46}$$

which is subjected to the following initial condition obtained by comparing eq. (36) and eq. (45)

$$a(\tau_m)=-\frac{Ste}{2K_s(1-\varepsilon_s)} \tag{47}$$

The location of the solid-liquid interface can be obtained by substituting eqs. (37) and (45) into eq. (25), i.e.,

$$\frac{dS}{d\tau}=\frac{2K_s}{1-S}\cdot a+\frac{Ste}{1-\varepsilon_s}\cdot erfc\left(\frac{Z-S_0}{2\sqrt{\tau-\tau_m}}\right) \tag{48}$$

Equations (45), (46) and (48) can be solved by the Runge-Kutta method.

3.2.3 Temperature distribution in the solid when $\beta>1$

Melting begins before the thermal penetration depth reaches to the bottom surface of the powder bed. The problem can be considered to be melting in semi-infinite mixed powder bed until the thermal penetration depth reaches the bottom of the powder bed. The solution for melting of an infinite powder bed contains mixture of two metal powders has been obtained by Zhang and Faghri [14]. The temperature distribution in the liquid phase is given by eq. (41).

The temperature distribution in the solid region is [14]

$$\theta_s(Z,\tau)=Sc\left[\left(\frac{\Delta-Z}{\Delta-S}\right)^2-1\right] \tag{49}$$

The location of solid –liquid interface is given by [14]

$$\frac{dS}{d\tau}=\frac{Ste}{1-\varepsilon_s}erfc\left(\frac{(1-\varepsilon_s)S}{2(1-\varepsilon_l)\sqrt{\tau-\tau_m}}\right)-\frac{2K_sSc}{\Delta-S} \tag{50}$$

The thermal penetration depth satisfies

$$\frac{d\Delta}{d\tau}=\frac{6K_s}{\Delta-S}\left(1+\frac{2}{3}Sc\right)-\frac{2Ste}{1-\varepsilon_s}erfc\left(\frac{(1-\varepsilon_s)S}{2(1-\varepsilon_l)\sqrt{\tau-\tau_m}}\right) \tag{51}$$

At the time that the thermal penetration depth reaches the bottom surface, i.e., $\Delta=1$, the temperature distribution in the solid is

$$\theta_s(Z,\tau_{\Delta=1})=Sc\left[\left(\frac{1-Z}{1-S}\right)^2-1\right] \tag{52}$$

The time that thermal penetration depth reaches to the bottom, $\tau_{\Delta=1}$, is obtained by

$$\Delta(\tau_{\Delta=1})=1 \tag{53}$$

When $\tau>\tau_{\Delta=1}$, the problem becomes melting in a finite slab. The temperature distribution in the solid, $\theta_s(Z,\tau)$, and the liquid-solid interface location, S, can be obtained by solving eq. (22), (23) and (24) with the integral approximate method that is identical with the situation when $\beta<1$.

4. RESULTS AND DISCUSSIONS

The effects of porosity, subcooling and dimensionless thermal conductivity and Stefan number on the surface temperature, locations of the liquid surface and solid-liquid interface of the powder bed will be investigated.

Fig. 2 shows how the surface temperature is influenced by the porosity in the liquid phase for $Ste = 0.02$ and different subcooling parameter. The effect of shrinkage is isolated by fixing the subcooling parameter, porosity of the solid phase, and dimensionless thermal conductivity. It can be seen that the surface temperature increases with the increasing porosity in the liquid phase because the effective thermal conductivity decreases with increasing volume fraction of the gas. When $Sc = 0.1$, the preheating time is much shorter compared with the case of $Sc = 3.0$. The effect of shrinkage on the surface temperature for $Ste = 0.15$ is shown in Fig. 3. As can be seen, the increase of porosity in the liquid phase also results in the increase of surface temperature and higher Sc requires a longer preheating time. When $Sc = 3.0$, one can observe the duration of the melting process is shortened significantly when Ste increases from 0.02 to 0.15.

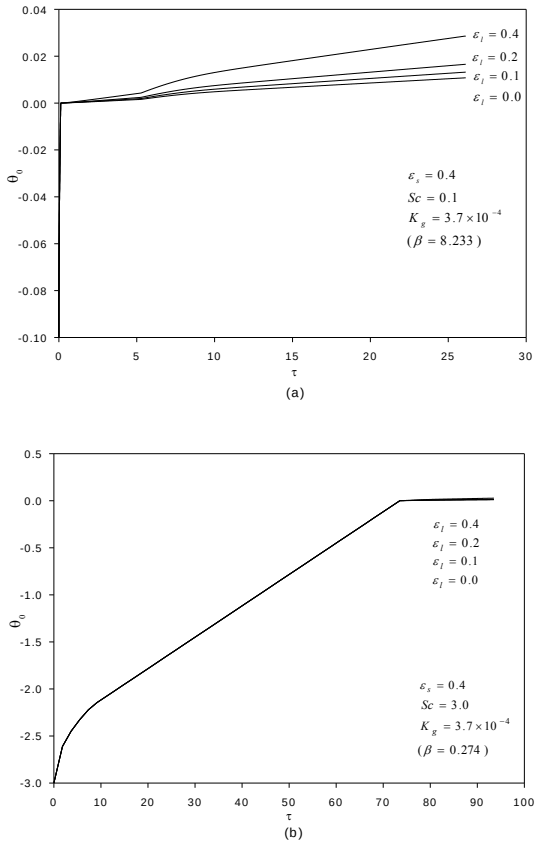

Fig.2 Effect of porosity in the liquid phase on surface temperature ($Ste = 0.02$)

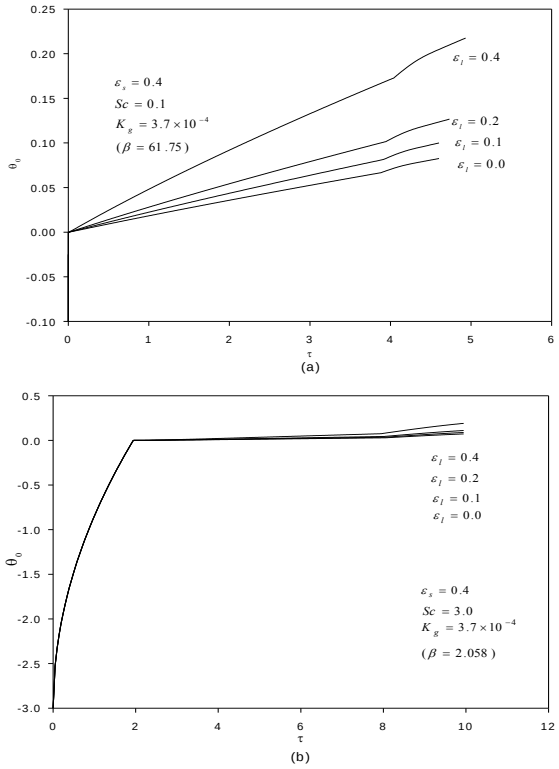

Fig.3 Effect of porosity in the liquid phase on surface temperature ($Ste = 0.15$)

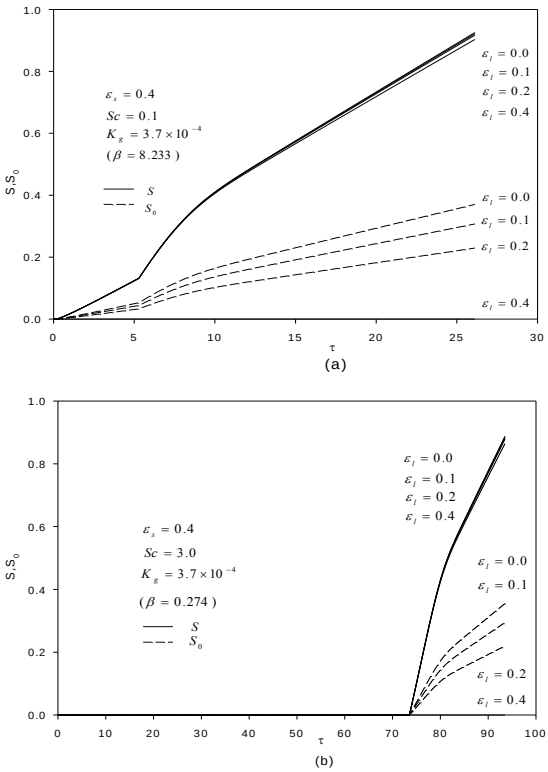

Fig.4 Effect of porosity in the liquid phase on the location of the liquid surface and liquid-solid interface ($Ste = 0.02$)

Fig. 4 shows the locations of solid-liquid interface and liquid surface corresponding to the conditions of Fig. 2. The solid-liquid interface moves faster when more gas is driven from the liquid. The corresponding location of the liquid surface moves downward significantly due to the shrinkage of the mixed metal powder bed. The locations of solid-liquid interface and liquid surface corresponding to the conditions of Fig. 3 are shown in Fig. 5. The decrease of porosity in the liquid phase also expedites the moving of the solid-liquid interface and liquid surface toward the bottom.

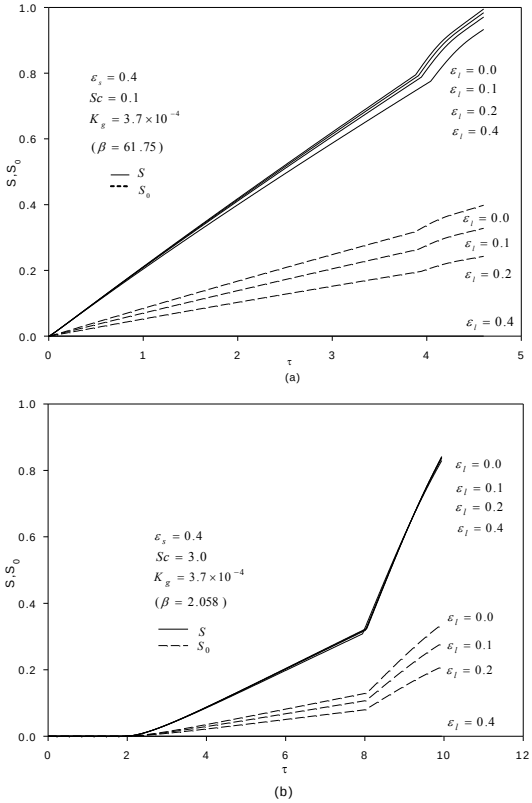

Fig.5 Effect of porosity in the liquid phase on the location of the liquid surface and liquid-solid interface ($Ste = 0.15$)

Fig. 6 shows the effect of the initial subcooling on the surface temperature for $Ste = 0.02$. It can be seen that the preheating time increases when the subcooling parameter, Sc, is increased from 0.1 to 0.5. The same trend is observed when Sc increases from 1.0 to 3.0. The effect of the initial subcooling on the surface temperature for $Ste = 0.15$ is shown in Fig. 7. Compared to the case of Ste=0.02, the preheating time for Ste=0.15 is significantly shortened. Meanwhile, the preheating time for Ste=0.15 increases when Sc increased from 0.1 to 3.0. Fig. 6(a) and Fig. 7 indicated that the lower liquid surface temperature is obtained for larger initial subcooling. However, these changes are not shown apparently in Fig. 6(b).

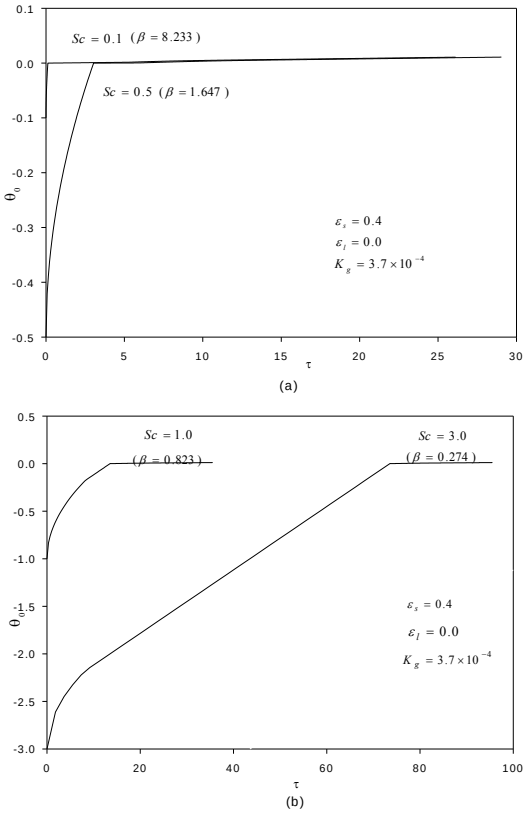

Fig.6 Effect of subcooling on surface temperature ($Ste = 0.02$)

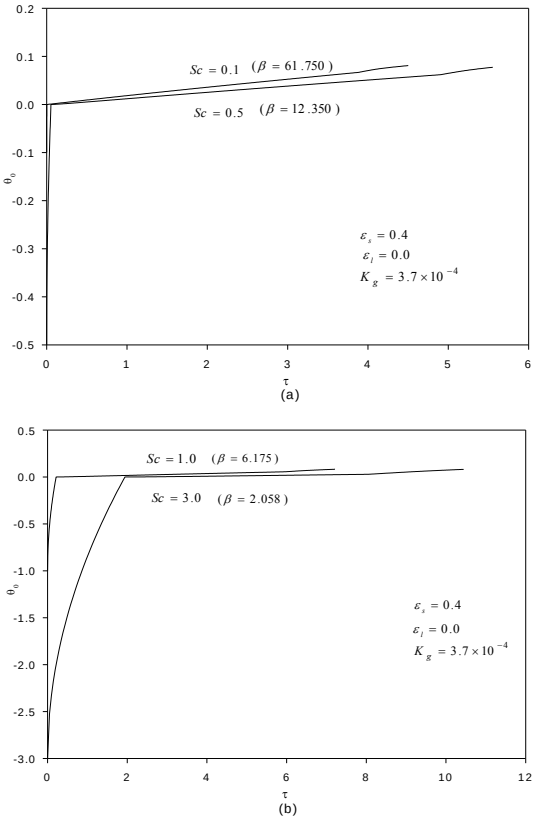

Fig.7 Effect of subcooling on surface temperature ($Ste = 0.15$)

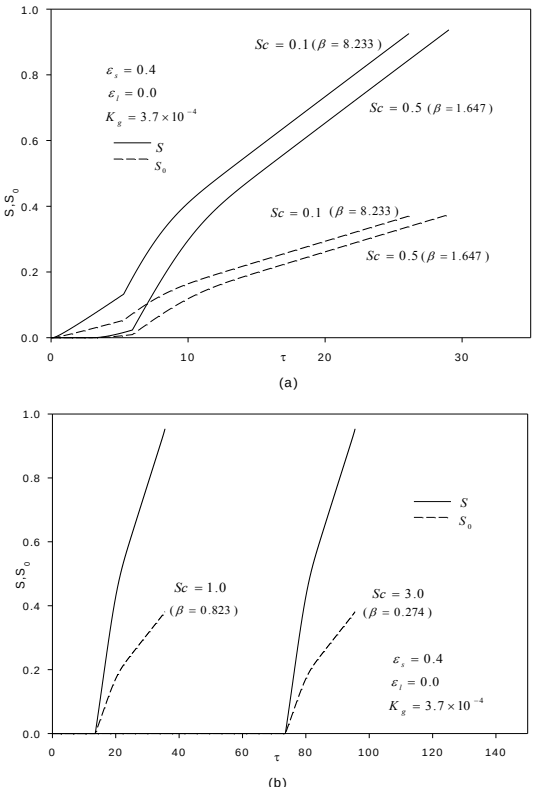

Fig.8 Effect subcooling on the location of the liquid surface and liquid-solid interface ($Ste = 0.02$)

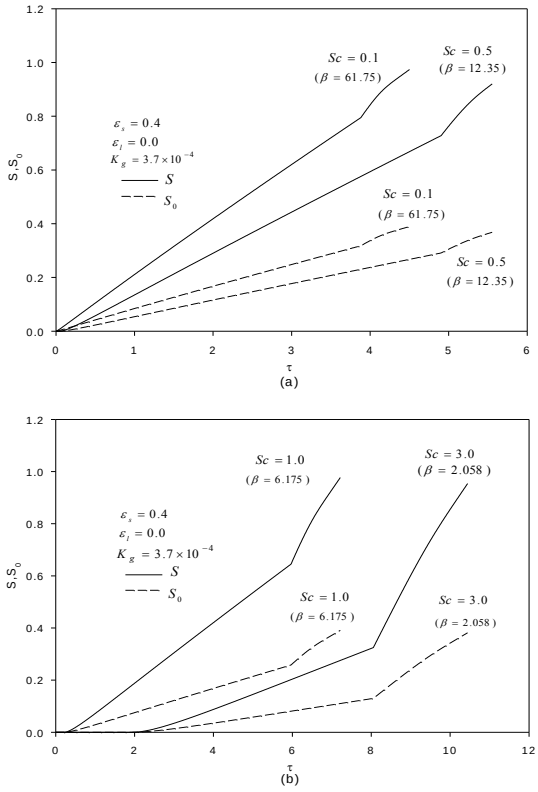

Fig.9 Effect subcooling on the location of the liquid surface and the liquid-solid interface ($Ste = 0.15$)

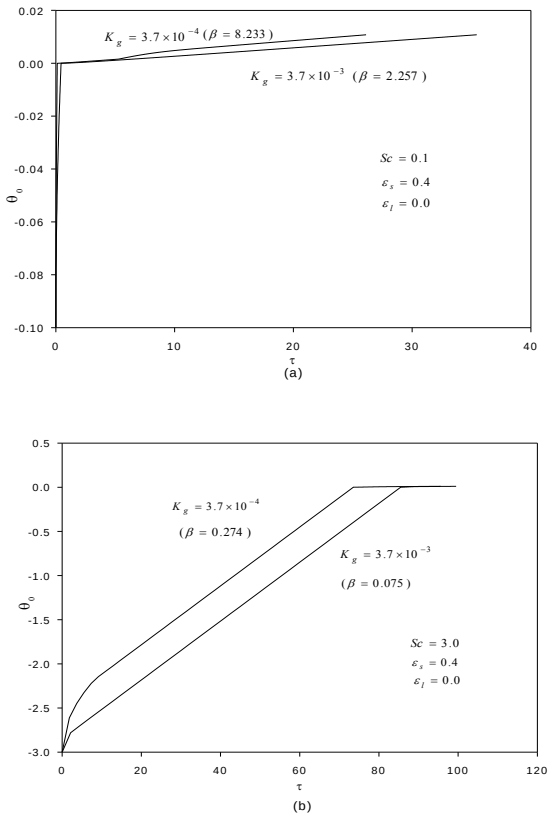

Fig.10 Effect of dimensionless thermal conductivity of gas on surface temperature ($Ste = 0.02$)

Fig. 8 shows the locations of solid-liquid interface and liquid surface corresponding to the conditions of Fig. 6. As can be seen in Fig. 8(a), the existence of initial subcooling reduces the moving velocity of the solid-liquid interface substantially. Before the thermal penetration depth reaches the bottom, the solid-liquid interface moves slowly and becomes faster after the thermal penetration depth has arrived at the bottom. At higher subcooling parameter, melting occurs only after the thermal penetration depth has reached the bottom as shown in Fig. 8(b). The reason about those phenomena is that the adequate preheating brings the average temperature of powder bed very close to the melting point of low melting powder so that the melting process can proceed quickly at the beginning. However, the relationship between the solid-liquid interface and liquid surface is the same for different subcooling parameters since it only depends on the volume fractions of the gas in the solid and liquid phase [see eq. (26)]. The locations of solid-liquid interface and liquid surface corresponding to the conditions of Fig. 7 are also plotted in Fig. 9. The similar trend can be observed just like what has happened in Fig. 8.

The dimensionless thermal conductivity of the gas has significant impact on the effective thermal conductivity of the powder bed [14]. The effect of dimensionless thermal conductivity of the gas on the surface temperature for $Ste = 0.02$ is shown in Fig. 10. It can be seen that the preheating time is increased when the thermal conductivity of the gas is increased. And the surface temperature is slightly lower for higher thermal

conductivity of the gas. While the effect of dimensionless thermal conductivity of the gas on the preheating time is insignificant when Sc=0.1, its effect is significant when $Sc = 3.0$. Fig. 11 shows the effect of dimensionless thermal conductivity of the gas on the surface temperature for $Ste = 0.15$. The effect of dimensionless thermal conductivity of the gas on the preheating time is insignificant for $Sc = 0.1$.

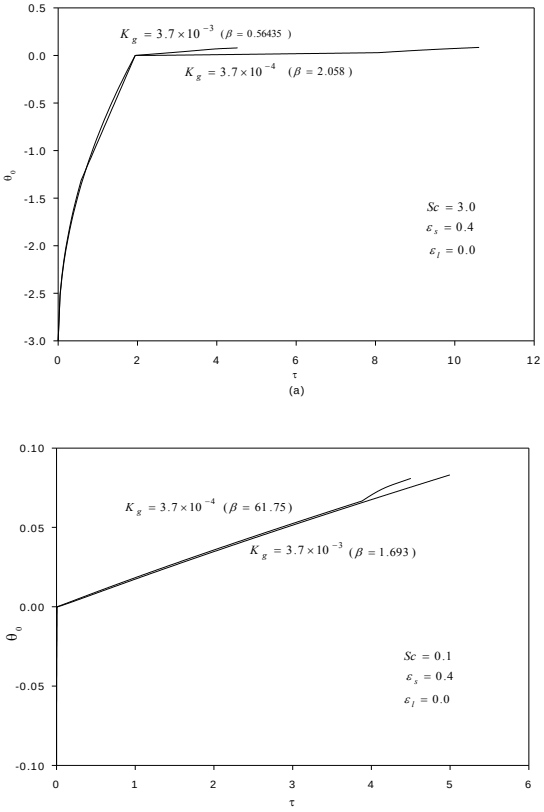

Fig 11 Effect of dimensionless thermal conductivity of gas on surface temperature ($Ste = 0.15$)

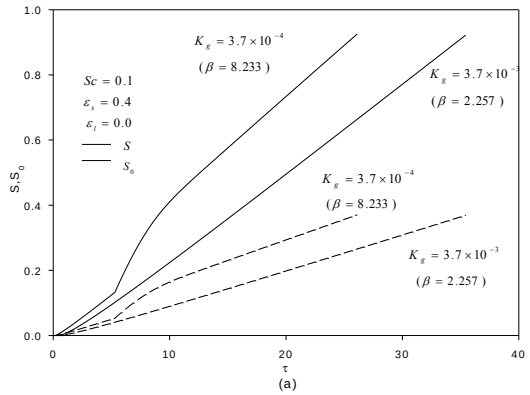

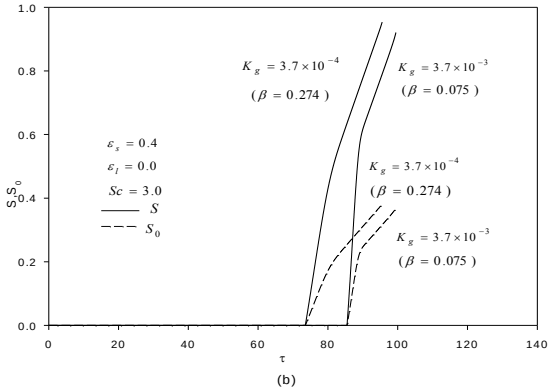

Fig.12 Effect of dimensionless thermal conductivity of gas on the location of the liquid surface and liquid-solid interface ($Ste = 0.02$)

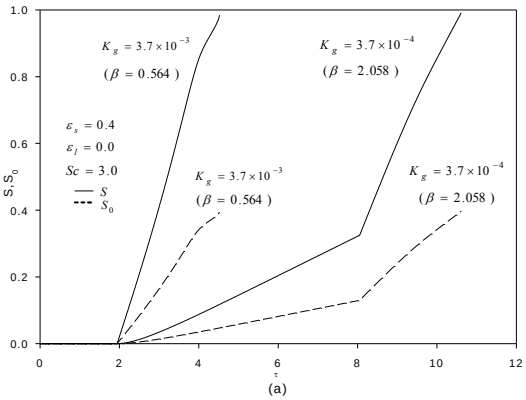

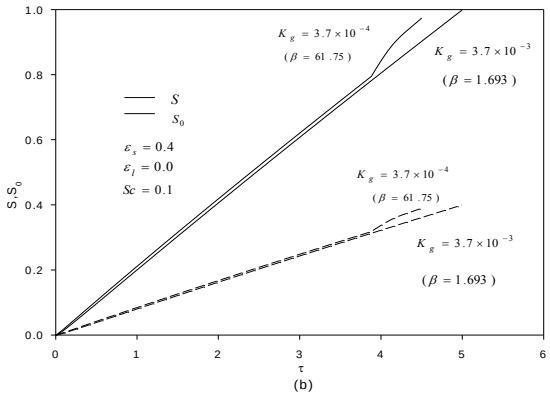

Fig.13 Effect of dimensionless thermal conductivity of gas on the location of the liquid surface and iquid-solid interface ($Ste = 0.15$)

The effect of dimensionless thermal conductivity of the gas on locations of solid-liquid interface and liquid surface corresponding to the conditions of Fig. 10 are shown in Fig. 12. As can be seen, the moving velocity of the solid-liquid interface decreases with increasing dimensionless thermal conductivity of gas. Fig. 13 shows the effect of dimensionless thermal conductivity of the gas on locations of solid-liquid interface and liquid surface corresponding to the conditions of Fig. 11. The solid-liquid interface with its corresponding liquid surface is

also slowed down by the higher dimensionless thermal conductivity of the gas. So the effect of the dimensionless thermal conductivity of gas on melting process is very significant.

5. CONCLUSION

Melting of a subcooled mixed metal powder bed with a finite thickness subjected to constant heat flux heating was investigated analytically. The shrinkage induced by melting was also taken into account. The increase of Stefan number and decrease of subcooling will accelerate the melting process significantly. Melting in a finite powder bed is different from melting in a semi-infinite space since the solid-liquid interface during melting in a finite powder bed moves more quickly than that in a semi-infinite space. The physical model and results of this investigation built solid foundation to study the complex three-dimensional selective laser sintering (SLS) process.

ACKNOWLEDGMENTS

Support for this work by the Office of Naval Research (ONR) under grant number 00014-02-1-0356 is greatly acknowledged.

REFERENCES

[1] Conley J.G. and Marcus H.L., 1997, "Rapid prototyping and solid freeform fabrication," *Journal of Manufacturing Science and Engineering,* **119,** pp. 811-816.

[2] Viskanta R., 1983, *Solar Heat Storage: Latent Heat Materials,* CRC Press, FL.

[3] Yao L. C. and Prusa J., 1989, "Melting and freezing," *Advances in Heat Transfer,* **25,** pp. 1-96.

[4] Eckert E. R.G. and Drake R. M., 1972, *Analysis of Heat and Mass Transfer*, McGraw-Hill, London.

[5] Crank J., 1956, *The Mathematics of Diffusion*, Clarendon Press, Oxford.

[6] Carslaw H.S. and J. C. Jaeger, 1959, *Conduction of Heat in Solids*, Clarendon Press, Oxford.

[7] Charach C. and Zarmi Y., 1991, "Planar solidification in a finite slab: effect of density change," *Journal of Applied Physics,* **70,** pp. 6687-6693.

[8] Zhang Y. Chen Z. Q. and Wang Q. J., 1990, "Analytical solution of melting in a subcooled semi-infinite solid with boundary conditions of the second kind," Presented at Procs. Int. Symp. on Manufacturing and Materials processing, Dubrovnik, Yugoslavia.

[9] Goodman T.R. and Shea J. J., 1960, "The melting of finite slabs," *Journal of Applied Mechanics,* pp. 16-25.

[10] Zhang Y. W. and Jin Y. Y., Chen Z. Q., Dong Z. F. and Ebadian M. A., 1993, "An analytical solution to melting in a finite slab with a boundary condition of the second kind," *ASME Journal of Heat Transfer,* **115**, pp. 463-467.

[11] Kim C. J. and Ro S. T., 1993, "Shrinkage formation during the solidification process in an open rectangular cavity," *Journal of Heat Transfer,* **115**, pp. 1078-1081.

[12] Manzur T., DeMaria T., Chen W., and Roychoudhuri C., 1996, "Potential role of high powder laser diode in manufacturing," presented at SPIE Photonics West Conference, San Jose, CA.

[13] Bunnell D.E., 1995, "Fundamentals of selective laser sintering of metals," Ph.D. dissertation, University of Texas at Austin.

[14] Zhang Y. and Faghri A., 1999, "Melting of a subcooled mixed powder bed with constant heat flux heating," *nternational Journal of Heat and Mass Transfer,* **42**, pp. 775-788.